

Experimental demonstration for scanning near-field optical microscopy using a metal micro-slit probe at millimeter wavelengths

Jongsuck Bae,^{a),b)} Tatsuya Okamoto, Tetsu Fujii, and Koji Mizuno^{b)}
*Research Institute of Electrical Communication, Tohoku University, 2-1-1 Katahira, Aoba-ku,
Sendai 980-77, Japan*

Tatsuo Nozokido
*Photodynamics Research Center, The Institute of Physical and Chemical Research (RIKEN),
19-1399 Aza-Koeji, Nagamachi, Aoba-ku, Sendai 980, Japan*

(Received 9 September 1997; accepted for publication 14 October 1997)

Scanning near-field optical microscopy using a slit-type probe is discussed. The slit-type probe has a width of much less than a wavelength, λ , and a length on the order of λ , and thus has high transmission efficiency. Two dimensional near-field images of objects have been constructed using an image reconstruction algorithm based on computerized tomographic imaging. Experiments performed at 60 GHz ($\lambda = 5$ mm) show that this type of near-field microscopy can achieve a spatial resolution of better than $\lambda/45$ for two dimensional imaging. A method for fabricating a submicron width slit probe at the end of an optical fiber is presented for extending this microscopy to optical waves. © 1997 American Institute of Physics. [S0003-6951(97)02250-X]

Scanning near-field imaging technologies have attracted much attention as a new optical technique to circumvent diffraction limits of about a half wavelength in conventional optics.^{1,2} In conventional near-field optical microscopes,^{3,4} tapered optical fiber probes with a submicroscopic aperture at the apex have been generally used because spatial resolution is determined primarily by the aperture size.⁵ In apertured probes with hole diameters less than $\lambda/10$ (λ : light wavelength), the transmission efficiency (or coefficient) is typically 10^{-7} or less for incident light power.⁶ This low transmission efficiency results in low probing sensitivity and becomes a serious problem, particularly in some applications such as spectroscopy of semiconductors measured in the illumination-collection hybrid mode⁷ and high density data storage where high probing power is required to speedily read and write data.⁸ For these near-field optics applications, a tapered metal micro-slit is proposed as a new near-field optical probe with high transmission efficiency.

Figure 1 shows the configuration of the metal micro-slit probe. The metal micro-slit is fabricated at the end of a tapered optical fiber. The slit width, d , is much less than λ , but the slit length, l , is larger than $\lambda/2$. Since the tapered slit probe acts as a simple parallel plate transmission line, cutoff effects,⁹ which largely decrease transmission power in apertured probes, do not occur. Therefore, the slit probe can achieve a higher transmittance even though d is much less than λ . From transmission line theory, it is found that the transmission efficiency for the slit probe is roughly proportional to d/λ , compared to $(d/\lambda)^{-6}$ for the ideal case of a circular aperture with a hole diameter of d .¹⁰ In this letter, we demonstrate two dimensional imaging with subwavelength resolution using the tapered slit probe at a millimeter wavelength,¹¹ and discuss the feasibility of optical near-field microscopy with the slit probe.

^{a)}Electronic mail: bae@riec.tohoku.ac.jp

^{b)}Also at: Photodynamics Research Center, The Institute of Physical and Chemical Research (RIKEN), 19-1399 Aza-Koeji, Nagamachi, Aoba-ku, Sendai 980, Japan.

As a different type of a slit probe, Golosovsky and Davidov¹² proposed a narrow resonant slit fabricated at the end of a metal rectangular waveguide for use in resistivity microscopy at millimeter wavelengths. Since the slit acts as a resonant slot antenna, the transmission efficiency can be nearly unity by choosing precisely the slit dimensions, even though the slit width approaches zero. However, resonance in the slit results in narrow bandwidth. In addition, applying the structure of the resonant slit to an optical probe would be difficult in practical fabrication.

Since the metal slit probe is a one dimensional near-field probe, two dimensional near-field images with subwavelength resolution cannot be generated by using conventional raster-scanning methods. This problem can be solved by using deconvolution techniques widely used in x-ray computerized tomography (CT).¹³

Experimental demonstrations for this method were carried out at a millimeter wave frequency of 60 GHz ($\lambda = 5$ mm). Figure 2 shows the experimental setup. The metal slit was fabricated at the end of a tapered rectangular waveguide. The slit dimensions were $d = 82 \mu\text{m}$ ($\sim \lambda/62$), $l = 4.8$ mm ($\sim \lambda$), and a taper angle of 30° . The waveguide with the slit probe, and a receiving horn antenna were connected to a WILTRON 360B vector network analyzer. An aluminum patch with dimensions of $0.9 \text{ mm} \times 0.75 \text{ mm}$ was

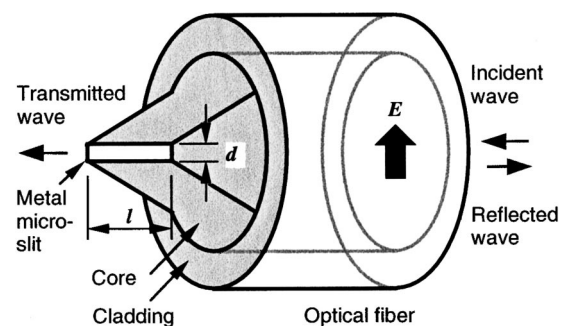


FIG. 1. Metal micro-slit near-field probe.

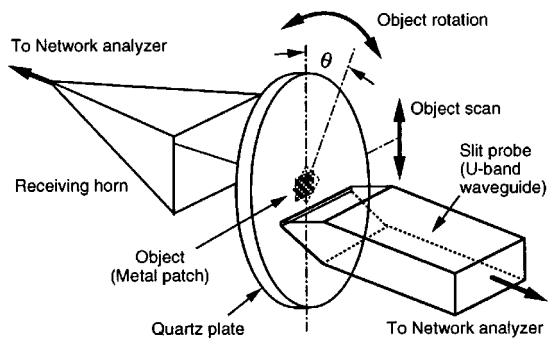


FIG. 2. Experimental setup for scanning near-field millimeter-wave microscopy using a metal slit probe.

used as an observation object. The metal patch was supported by a quartz plate with a thickness of 1.87 mm.

The metal patch was scanned linearly for different objection-rotation angles, θ , as shown in Fig. 2. For each scan step, transmittance and reflectance were simultaneously measured by the network analyzer which executes phase-sensitive heterodyne detection. This scan method is quite different from the raster scan method used in conventional near-field microscopes. Two dimensional images of the metal patch were reconstructed from each set of measured data, i.e., the vector signals in reflection or transmission, by using an image reconstruction algorithm based on computerized tomographic imaging.¹⁴

Figure 3 compares the optical image (a) and the reconstructed image (b) of the metal patch measured in reflection mode. Experimental parameters used in this experiment were as follows. The field of view was 2.1 mm. For linear motion

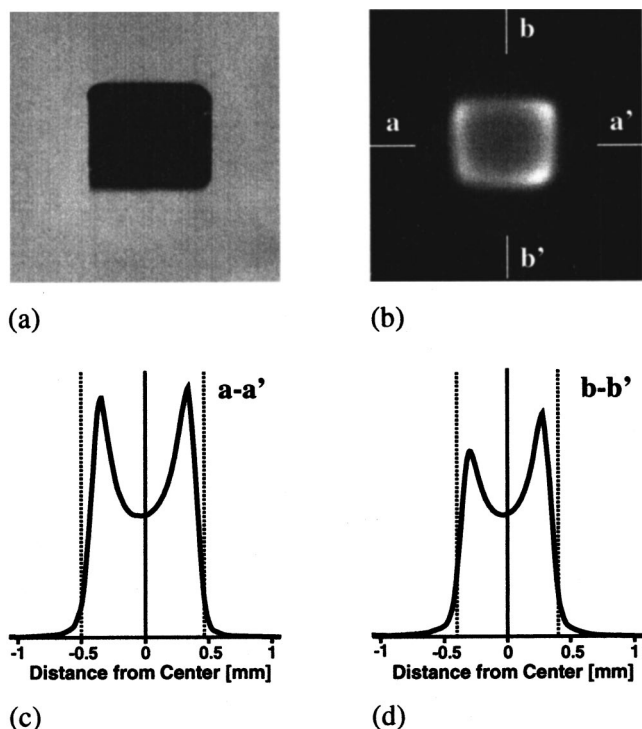


FIG. 3. Comparison of images of a metal patch at 60 GHz: (a) optical image, (b) reconstructed near-field image in reflection mode. (c) and (d) are one dimensional intensity variations along the line $a-a'$ and line $b-b'$ in (b), respectively. The dotted lines in (c) and (d) indicate the actual width (0.9 mm) and length (0.75 mm) of the metal patch, respectively.

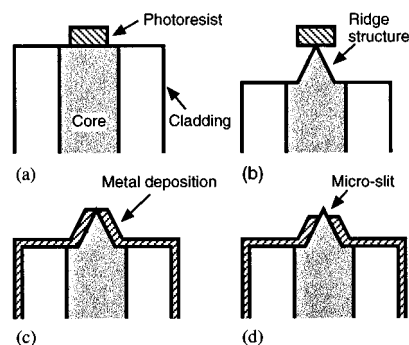


FIG. 4. Process sequence for the fabrication of a metal micro-slit at the end of an optical fiber: (a) after patterning photoresist with dimensions of $30 \mu\text{m} \times 10 \mu\text{m}$; (b) after etching the optical fiber in $\text{HF}:\text{NH}_4\text{F}$ ($=1:6.5$); (c) after evaporating metal at a right angle to the desired slit surface; (d) after wet chemical etching of the metal coated ridge structure to open a slit aperture.

the sampling interval and total sampling number were $48 \mu\text{m}$ and 63 points, and for rotational motion they were 5.81° and 31 points, respectively. Probe-to-object separation was about $10 \mu\text{m}$. Figures 3(c) and 3(d) show the intensity variations along the lines $a-a'$ and $b-b'$ indicated in Fig. 3(b), respectively. From these results, the spatial resolution has been estimated to be about $110 \mu\text{m}$ ($\sim \lambda/45$). Similar results were obtained in transmission mode. Those experimental results show that two dimensional imaging with subwavelength resolution is possible in a near-field microscopy using the slit probe.

In a near-field microscopy using an image reconstruction algorithm, it should be noted that heterodyne detection must be chosen for signal measurement when the same coherent waves are used for both illumination and detection. CT imaging requires projection data which are simple integrations of scattered waves from an object at different positions on a straight line path through the object. In conventional CT imaging, incoherent scattered waves are required for image reconstruction because they preserve the relationship between the measured data and the corresponding positions along the object's cross section.¹⁴ However, a coherent source, such as a laser, is commonly used for near-field microscopy. In this case, interference between scattered waves from an object at different positions along a straight line path, (in our case the length of the slit) breaks up the relationship. In order to remove the interference effect from the measured signals

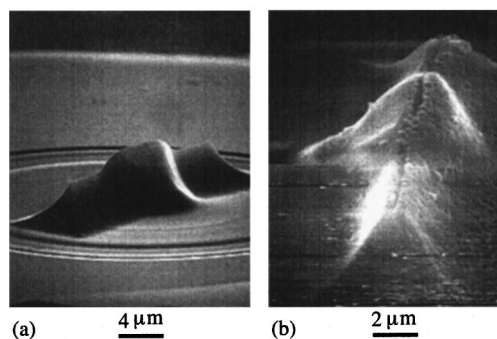


FIG. 5. A metal micro-slit fabricated at the center of the end of a single-mode optical fiber: (a) ridge structure with a taper angle of 80° , (b) metal slit with a width of 270 nm fabricated on the ridge structure.

(i.e., the projection data), heterodyne detection must be used. This is the reason why we have used a vector network analyzer in the experiment. In a case where the signal waves are incoherent, such as in photoluminescence measurements of objects, direct detection could be used.

For extending this near-field microscopy to the optical region, a metal micro-slit probe with submicron width (shown in Fig. 1) is required. In order to fabricate such slit probes, a chemical etching technique was successfully adopted.¹⁵ The fabrication process used here is shown in Fig. 4. This fabrication method is almost the same as that for conventional probes,¹⁶ except for the photolithographic process. In Fig. 4(d), the slit width must be controlled by adjusting the etching time because the metal thickness at the top of the ridge is thinner than that at other places.

Figure 5 shows the ridge structure fabricated at the center of the core of an optical fiber with a 125 μm diameter (a), and the same ridge after etching a 270 nm width metal slit (b). The ridge structure has a length of 5.5 μm for a core diameter of 8.8 μm , a height of 7.2 μm , and a taper angle of 80°. Both the flatness along the length of ridge and the radius of curvature at the top of the ridge are less than 30 nm. The radius of curvature is comparable to that of conventional apertured probes with hole diameters of several tens of nanometer.⁴ In Fig. 5(b), the coating metal is aluminum and its thickness is about 300 nm. Another probe with a 180 nm width slit was fabricated using gold instead of aluminum as a coating metal, through the same fabrication process. These results show that a metal slit probe with a sub-micron width can be fabricated by chemical etching. These probes can be used in near-field microscopy in the near-infrared region.

In order to fabricate slit probes with narrower width, a smaller taper angle than 80° for the ridge structure is required, to make precise fabrication of the slit through chemical etching. A ridge structure with a smaller taper angle of about 20° could be fabricated by choosing an optical fiber with a higher doped core and the appropriate etching solution, in a way similar to how conventional probes with nanometric apertures have been fabricated.¹⁷

In conclusion, we have proposed scanning near-field op-

tical microscopy using a slit-type probe. Experiments performed at a wavelength of 5 mm show that scanning slit near-field microscopy can perform two dimensional imaging with a spatial resolution of 110 μm by utilizing a deconvolution technique. We have shown that a metal micro-slit probe with submicron width for use in optical microscopy can be fabricated by using a chemical etching technique. These results indicate that near-field microscopy using a slit probe has potential as a near-field imaging technique over a wide range of electromagnetic spectra, from millimeter through optical wavelengths.

The authors would like to acknowledge Professor M. Ohtsu at Tokyo Institute of Technology for helpful discussions. This work was partially supported by a Grant-in-Aid for Scientific Research on Priority Areas from the Ministry of Education, Science, Sports, and Culture, Japan.

¹D. W. Pohl, W. Denk, and M. Lanz, *Appl. Phys. Lett.* **44**, 651 (1984).

²A. Harootunian, E. Betzig, M. Isaacson, and Lewis, *Appl. Phys. Lett.* **49**, 674 (1986).

³E. Betzig and J. K. Trautman, *Science* **257**, 189 (1992).

⁴R. U. Maheswari, H. Tatsumi, Y. Katayama, and M. Ohtsu, *Opt. Commun.* **120**, 325 (1995).

⁵E. H. Synge, *Philos. Mag.* **6**, 356 (1928).

⁶G. A. Valaskovic, M. Holton, and G. H. Morrison, *Appl. Opt.* **34**, 1215 (1995).

⁷T. Saiki, M. Mononobe, and M. Ohtsu, *Appl. Phys. Lett.* **68**, 2612 (1996).

⁸E. Betzig, J. K. Trautman, R. Wolfe, E. M. Gyorgy, P. L. Finn, M. H. Kryder, and C.-H. Chang, *Appl. Phys. Lett.* **61**, 142 (1992).

⁹E. L. Buckland, P. J. Moyer, and M. A. Paesler, *J. Appl. Phys.* **73**, 1018 (1993).

¹⁰U. Dürig, D. W. Pohl, and F. Rohner, *J. Appl. Phys.* **59**, 3318 (1986).

¹¹T. Nozokido, J. Bae, T. Fujii, M. Ito, and K. Mizuno, *Conference Digest of 22th International Conference Infrared and Millimeter Waves, 1997*, p. 302.

¹²M. Golosovsky and D. Davidov, *Appl. Phys. Lett.* **68**, 1579 (1996).

¹³M. Golosovsky, A. Galkin, and D. Davidov, *IEEE Trans. Microwave Theory Tech.* **44**, 1390 (1996).

¹⁴A. C. Kak and M. Slaney, *Principles of Computerized Tomographic Imaging* (IEEE, New York, 1988), pp. 49–77.

¹⁵T. Miyajima, J. Bae, T. Akizuki, S. Okuyama, and K. Mizuno, *Conference Digest of 19th International Conference on Infrared and Millimeter Waves, 1994*, p. 153.

¹⁶T. Pangaribuan, S. Jiang, and M. Ohtsu, *Electron. Lett.* **29**, 1978 (1993).

¹⁷M. Ohtsu, *J. Lightwave Technol.* **13**, 1200 (1995).